



AME0006

Deterioration diagnosis of Li-ion battery with AC impedance measurement analysis

Toshiyuki Sakamoto*

Department of Prime Mover Engineering, School of Engineering, Tokai University,
4-1-1 Kitakaname, Hiratsuka city, Kanagawa pref., 259-1292 Japan

* Corresponding Author: E-mail : toshiya_sakamoto@tokai-u.jp

Abstract. Secondary battery is widely installed on an electric prime mover as the traction energy storage. The battery has a chemical degradation with cycle and preservation lifetime. The battery may reach to the lifetime in short of the design life on the different kinds of real world conditions which provide inconvenience to drive a vehicle and lead to some troubles of the power train system. It is important subject to detect the battery deterioration condition with convenient method and to build the verification technology of the battery to the deterioration. This study noticed at the battery impedance of both a resistance part and a capacitance part that can be measured at the same time by an AC impedance response analysis, one of the convenient method is available to verify the battery deterioration condition in progress of cycle life. The previous report was focused on a Nickel-metal hydride (Ni-MH) battery which is widely used as traction energy storage in Hybrid electric vehicles (HEVs), and apply the AC impedance response analysis to verify the battery deterioration. This study investigates a possibility extent that the AC impedance response analysis, which method is available to verify a Lithium ion (Li-ion) battery being exchanged from the Ni-MH battery, applies to the battery deterioration condition in progress of cycle lifetime experiment. The Li-ion battery cycle lifetime experiment progresses on the way, and this report explains the battery condition on the deterioration and verifies the Li-ion battery deterioration characteristics to the Ni-MH battery one.

1. Introduction

An environmentally friendly automobile, e.g. EVs and HEVs, have been developed and spreaded widely of that in all over the country. The EVs and HEVs have mechanical and electrical drivetrains with energy storage of batteries which must be considered in their lifetime^[1]. The energy storage of batteries are connected in series and which are installed on-board. In each battery cell which does not have the same charge-discharge characteristics along with the deterioration which gets out of durability service in short of the designing lifetime. The battery condition and deterioration are technically difficult to diagnosis in precisely.

This study challenges an on-board diagnosis technology to investigate the battery condition and deterioration, approaching in easy method which is an AC impedance measurement analysis. AC impedance measurement method applied to the battery, has an appropriate potential to verify the relations between the AC impedance and the battery capacity, to verify the relations between the battery the AC impedance and the battery temperature^[2]. The study object is set a quantitative research that verifications between the battery AC impedance characteristics and the battery

deterioration, which makes the battery condition and deterioration quantify in easily. The battery has a chemical degradation with cycle and preservation lifetime^[3]. The preservation lifetime is a battery deterioration along with the preservation time in which the battery leaves to stand. The preservation lifetime is a fundamental important because the whole life of EVs and HEVs occupies not in their drive conditions but in their park conditions. The preservation lifetime is a battery deterioration along with the preservation time in which the battery leaves to stand. The cycle lifetime is a battery deterioration along with the cumulative load in which the battery operates in charge-discharge cyclic load. EVs and HEVs have the charge-discharge cyclic mode but EVs and plug-in HEVs (plug-in hybrid electric vehicles, PHEVs) have charge mode by the way of external power source.

2. Experimental Method

2.1 Batteries used in the experiment

The experimental battery of which commercial model of cylindrical type Li-ion secondary batteries, the batteries have 2150mAh of rated capacity, are used for the experiment (model: UR18650A) manufactured by Sanyo Electric Co., Ltd. The experiment is carried out on brand-new batteries after activation by 10 charge-discharge cycles.

2.2 Batteries structure

A charge-discharge reaction of Li-ion experimental battery is the slow Lithium ion transfer process which is reversible conversion reaction between positive and negative electrode via electrolyte. The positive electrode material is used a metal oxide compound, e.g. cobalt, nickel, manganese and iron phosphate, with Lithium. The negative electrode material is used a carbo-based material.

2.3 Batteries reaction

A discharge reaction of Li-ion experimental battery is that the Lithium-ion placed an inter-layer of the carbo-based material of negative electrode transfers to the metal oxide compound with Lithium material of positive electrode, and electron from the negative electrode transfers to the positive electrode which works as a load current. The reaction equations are shown in Equation (1)-(3).

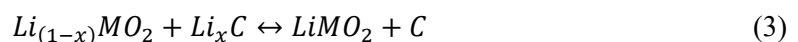
The positive electrode reaction is



The negative electrode reaction is



The total electrode reaction is



Where

Li: Lithium salt that can effectively passivate both negative and positive electrodes

x: reversible conversion reaction rate of Lithium salt

e⁻: electron transfer

C: carbonate for negative electrode, e.g. ethylene carbonate (EC) which has formed as a stable passivation film of a solid electrolyte interphase (SEI) suppressing further electrolyte decomposition
M: metallic element

2.4 AC impedance measurement method

AC impedance measurement method is to quantify interface structures of the battery storage, to measure battery AC impedance and battery phase difference between a cyclic wave from a signal oscillator and an AC current through the battery. The battery AC impedance and battery phase difference of battery impedance spectrum is measured by changing with the cyclic wave frequency from the signal oscillator.

2.5 Equivalent circuit theory

Battery impedance spectrum is plotted on the complex plane, which can be analyzed by combining impedances. Battery AC impedance has real (Z') and imaginary (Z'') parts plotted on the horizontal and vertical axes, respectively. The plotted figure is commonly called "Nyquist diagram". Figure 1 shows equivalent circuit of battery electrochemical impedance resistor (R) and capacitance (C) model. Equation (4) shows battery chemical impedance Z for the model in figure 1^{[4],[5]}.

$$Z = R_{sol} + \frac{R_{ct}}{1 + j\omega R_{ct} C_{dl}} \quad (4)$$

Z in Equation (1) consists of a real (Z') and imaginary (Z'') parts shown in Equations (5) - (8).

$$Z = Z' - jZ'' \quad (5)$$

$$Z' = R_{sol} + \frac{R_{ct}}{1 + \omega^2 R_{ct}^2 C_{dl}^2} \quad (6)$$

$$Z'' = \frac{\omega R_{ct}^2 C_{dl}}{1 + \omega^2 R_{ct}^2 C_{dl}^2} \quad (7)$$

$$\left(Z' - R_{sol} - \frac{R_{ct}}{2} \right)^2 + Z''^2 = \left(\frac{R_{ct}}{2} \right)^2 \quad (8)$$

where

- R_{sol} : solution resistance
(battery electrolyte resistance)
- R_{ct} : charge transfer resistance
- C_{dl} : electric double layer capacitance

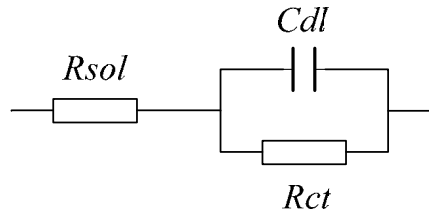


Figure 1. Basic RC model of battery chemical impedance.

2.6 Experimental method

The experimental study starts after the conditioning of battery is done with charge-discharge cyclic electrical load to the experimental battery by load control unit (type; HJ0610SD8Y) manufactured by Hokuto Denko Co., Ltd. The load control unit has a multi-channel to control which makes multi experimental battery conduct simultaneously. The temperature of experimental battery is measured by memory logger unit (type; 8423) manufactured by Hioki Co., Ltd. The AC impedance response with sweeping frequency was measured by chemical impedance analyser (model: IM3590) manufactured by Hioki Co., Ltd. The temperature of experimental battery is set in a thermostatic chamber (model: LU-113) manufactured by Espec Co., Ltd. And also, the temperature around standard band of 25 degC is set in a cool incubator (model: CN-40A) manufactured by Mitsubishi Engineering Co., Ltd. Figure 2 shows the load control and data logging system for experimental batteries.

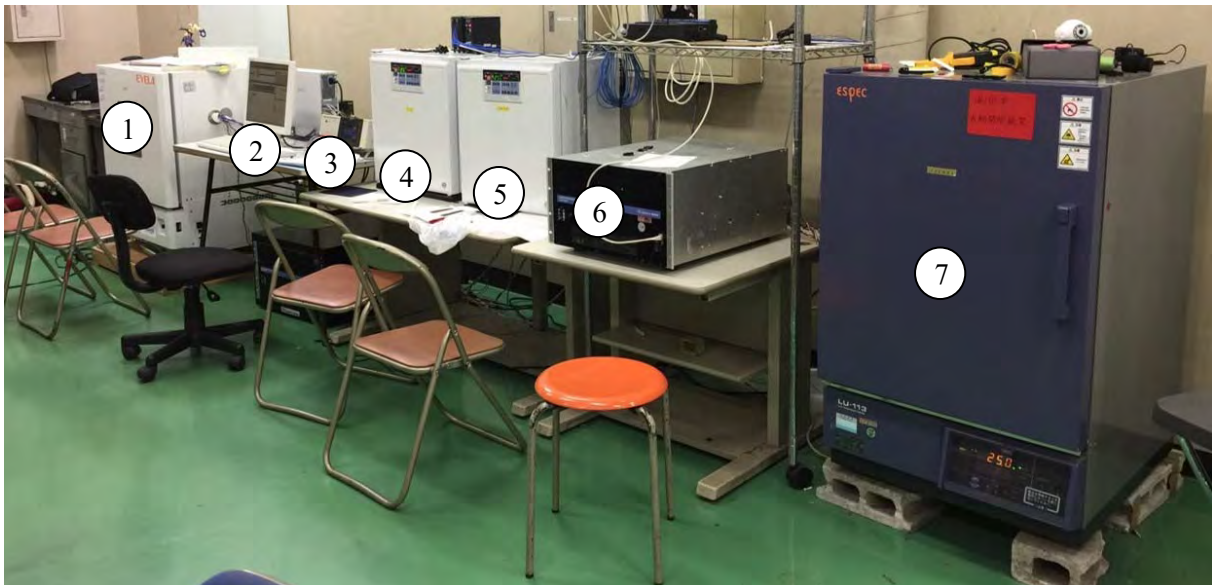


Figure 2. Load control and data logging system for experimental batteries, 1) thermostatic chamber 1, 2) computer system for load control and data logging, 3) AC impedance measurement unit, 4) cool incubator 1, 5) cool incubator 2, 6) power supply unit for charge-discharge load control, 7) thermostatic chamber 2.

The experimental load of the battery is shown in figure 3. The load profile was set on JC08 mode. Experimental battery load level was scales down to the actual current load profile of EVs and PHEVs with electric drive mode driving in JC08 mode. Thus, the experimental battery load was set within 60% to 40% SOC of the battery repeating the JC08 mode current profile shown on figure 3. One cycle of the battery experiment consists of JC08 load for 20% discharge and a constant current of 1125 mA (0.5 C) is given for 20% charge. Three samples of experimental batteries were done to with charge-

discharge cyclic electrical load for the initial conditioning. After the initial conditioning, the charge-discharge cyclic electrical load was applied to the experimental battery which was counted up from the zero cycle.

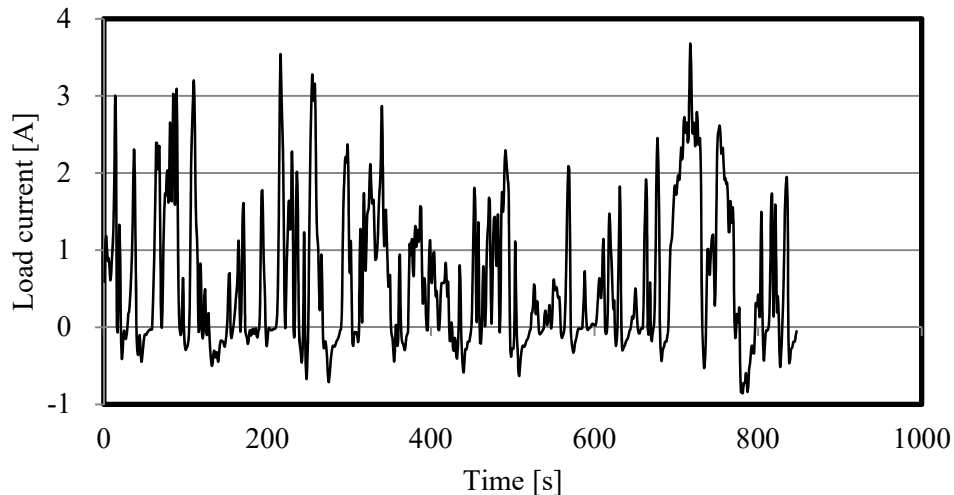


Figure 3. Experimental battery cycle load profile (JC08).

The measurement of AC impedance of the batteries under experiment has been done when experimental cycles are reaching checkpoint cycle. The measurement was carried out after the following process. First, the experimental battery was charged to the full capacity level and was preserved for 12 hours to reach stable state. Then the experimental battery was connected to the measurement wire harness by soldering to prevent voltage drop on the contact resistance^{[6], [7], [8]}. This is needed because battery impedance is significantly small in the range of few milliohms, and reducing any ohmic loss during AC impedance measurement is a necessity. For the AC impedance measurement, wires are soldered to both terminals of the battery and inserted into the test fixture (model: 9261-10) manufactured by Hioki Co., Ltd. To acquire appropriate data each measurement was performed three times. Battery AC impedance response was measured at different frequencies applied to the battery.

The AC impedance measurement was done for the frequencies in the range of 1000 Hz to 0.1 Hz. In the frequency range of 1000 Hz to 100 Hz, with 100 Hz step, in 100 Hz to 10 Hz range with 10 Hz step, and with 1 Hz and 0.1 Hz steps in the frequency ranges of 10 Hz to 1 Hz and 1 Hz to 0.1 Hz, respectively. The results of the AC impedance measurement for both batteries reveal both the real (Z') and the imaginary (Z'') components of impedance.

After the measurement, the experimental battery was discharged with constant current of 1125 mA (0.5 C) to the empty capacity level of 1.0 V and then charged for two hours with constant current of 1125 mA (0.5 C) to the full capacity. The resulted voltage curve of the battery nearly follows CC-CV (constant current – constant voltage) curve of standard charging method.

3 Experimental study

3.1 AC impedance response in cycle durability test^[10]

Figures 4-6 show the AC impedance measurement results for Li-ion experimental batteries. Three sets of brand new batteries were used for cycle durability test. AC impedance measurement has been done

first at the battery activation stage (0 cycle) and then after reaching each checkpoint cycle: 15, 50, 100, 400, 700 and 1000. The batteries measurement AC impedance results were increased and the batteries measurement results plot over almost the same trace area along with the durability experiment cycles progress.

Figures 4-6 show the chemical impedance transition with durability cycles, owing to increase impedance part of equivalent circuit (figure 1) parameters of Li-ion battery. On figures 4-6 electrolyte resistance (R_{sol}) and charge transfer resistance (R_{ct}) values are shown on the real part axis and electric double layer capacitance (C_{dl}) is shown on the imaginary part axis. Over the course of durability test cycles R_{sol} , R_{ct} and C_{dl} are eventually increased.

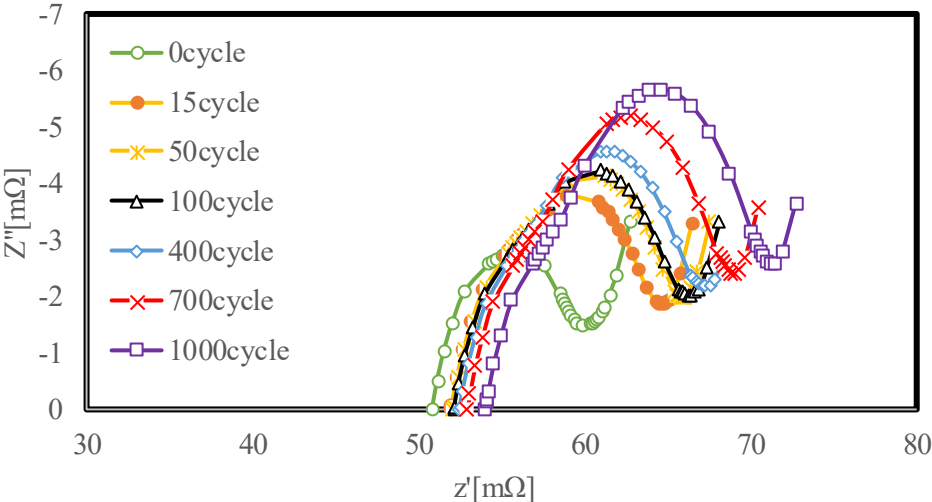


Figure 4. AC Impedance spectroscopy (Experimental sample L1).

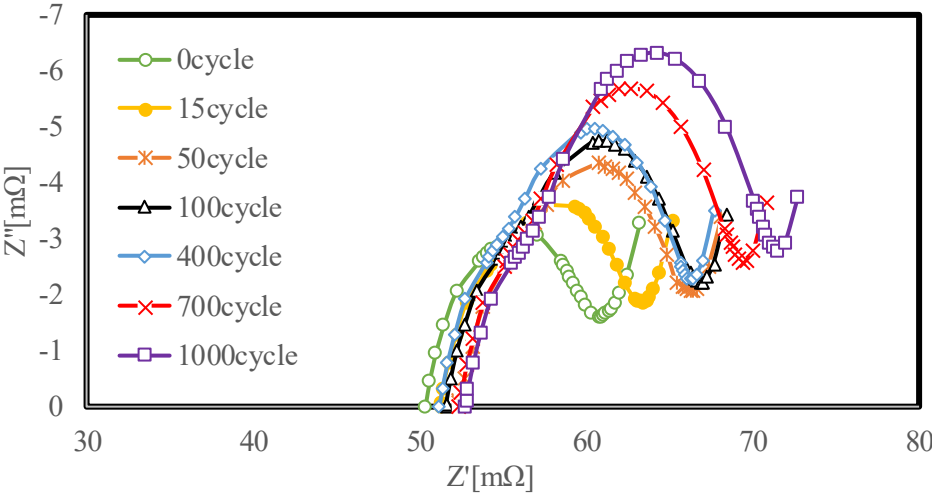


Figure 5. AC Impedance spectroscopy (Experimental sample L2).

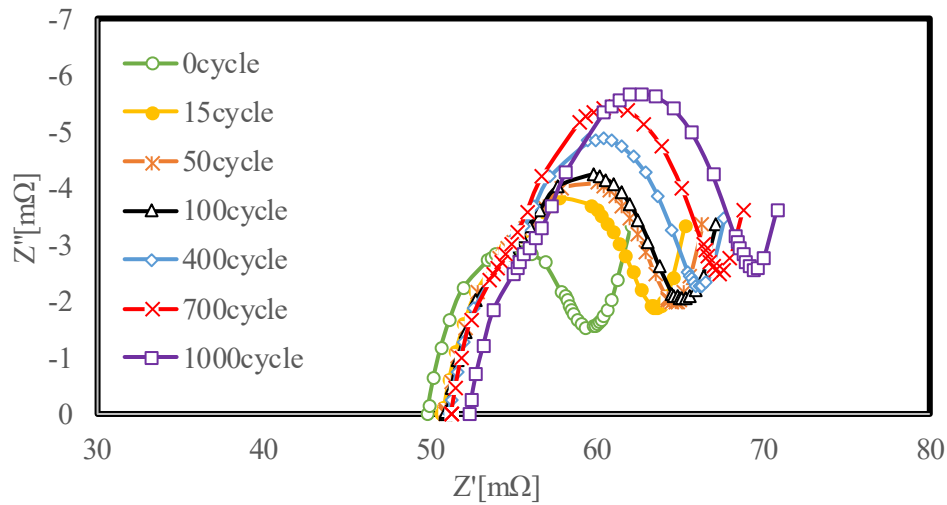


Figure 6. AC Impedance spectroscopy (Experimental sample L3).

3.2 Battery capacity in cycle durability test ^[9]

Figure 7 shows the experimental battery discharge capacity which was measured for the complete discharge check in each 300 cycle after 100 cycle, which was done in 100, 400, 700 and 1000 cycle. Before 100 cycle, checking cycle was much short span, in which activation (0 cycle), 15 and 50 cycle. The experimental Sample L3 was the most deterioration battery in all and the second deterioration was Sample L2 and the third place was Sample L1. The experimental battery discharge capacity was measured for the complete discharge check when the experimental battery was charged from empty to full capacity in advance of the measurement test.

Figure 8 shows the experimental battery discharge capacity which was measured from the start SOC of durability cycle in each 300 cycle after 100 cycle, which was done in 100, 400, 700 and 1000 cycle. Before 100 cycle, checking cycle was much short span, in which activation (0 cycle), 15 and 50 cycle. The experimental Sample L3 was the most dischargeable battery in all and the second dischargeable battery was Sample L2 and the third place was Sample L1. The experimental battery discharge capacity was measured from the start SOC of durability cycle when the experimental battery was charged from empty to full capacity and then discharged to 60% SOC (= the start SOC of durability cycle) in advance of the measurement test.

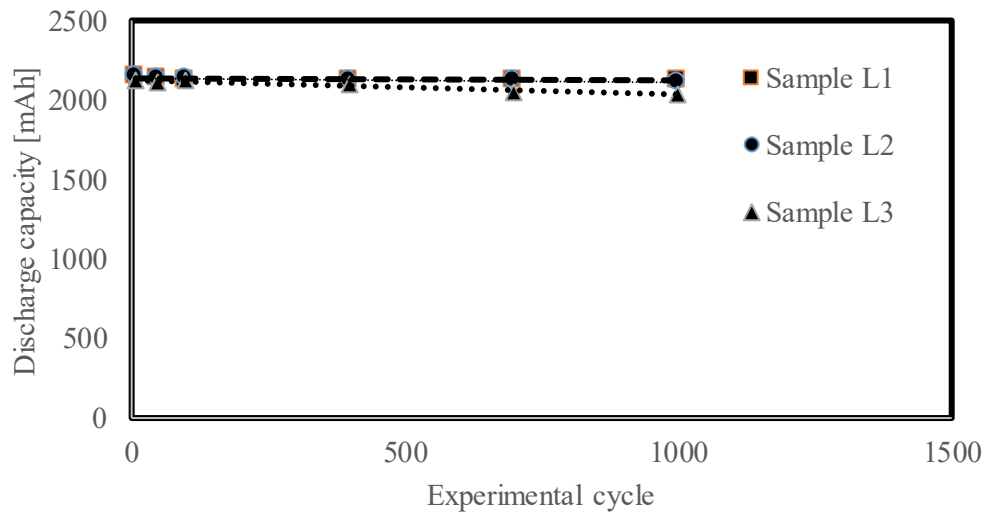


Figure 7. Battery discharge capacity (100%).

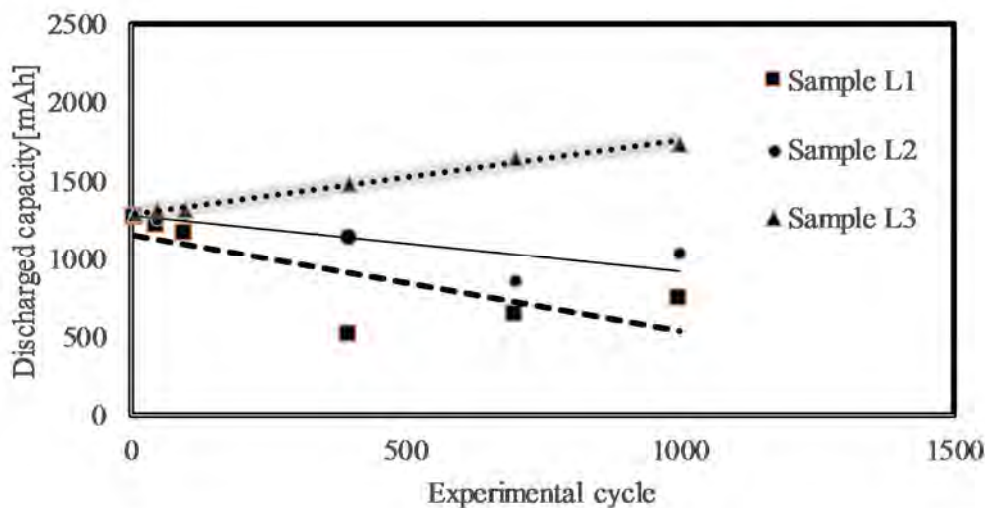


Figure 8. Battery discharge capacity (60%).

Figure 7 shows the battery deterioration was advanced from the initial capacity, 2150mAh (=100%SOC). Sample L1 was 1.1% deterioration, Sample L2 was 1.8% and Sample L3 was 5.1% at 1000 cycle. Figure 8 shows the durability cycle start SOC was changed from the initial SOC, 1290mAh (=60%SOC). Sample L1 shifted to 33%SOC, Sample L2 shifted to 49%SOC and Sample L3 shifted to 72%SOC from 100 cycle to 1000 cycle in average. In progressed durability cycle, the battery was deteriorated. In case of the battery capacity changes from initial capacity to an actual capacity, durability cycle start SOC is also changed to actual SOC of which actual capacity basement. Sample L1 shifted to 33%SOC, Sample L2 shifted to 50%SOC and Sample L3 shifted to 75%SOC from 100 cycle to 1000 cycle in average. The durability cycle specifies that discharge amount is 20% battery capacity from 60%SOC to 40%SOC. In actual durability test, sample L1 was under low SOC range of 33/13%SOC, sample L2 was middle SOC range of 50/30%SOC and sample L3 was high SOC range of 75/55%SOC, which made difference deterioration of the experimental batteries. The high SOC range of 75/55%SOC is much affected deterioration than the low SOC range of 33/13%SOC, which was 4.6 times (=5.1/1.1%) decreased from initial battery capacity in 1000 cycle.

3.3 Battery exhaust voltage in cycle durability test

Figure 9 shows the experimental battery voltage at the mode end of the durability cycle discharge which plots in figure each 100 cycle. The experimental Sample L3 was the highest voltage transition battery in all and the second battery was Sample L2 and the third place was Sample L1. The above result shows that the higher voltage battery at the mode end of the durability cycle discharge is the larger amount of battery capacity in the start SOC of the durability cycle discharge.

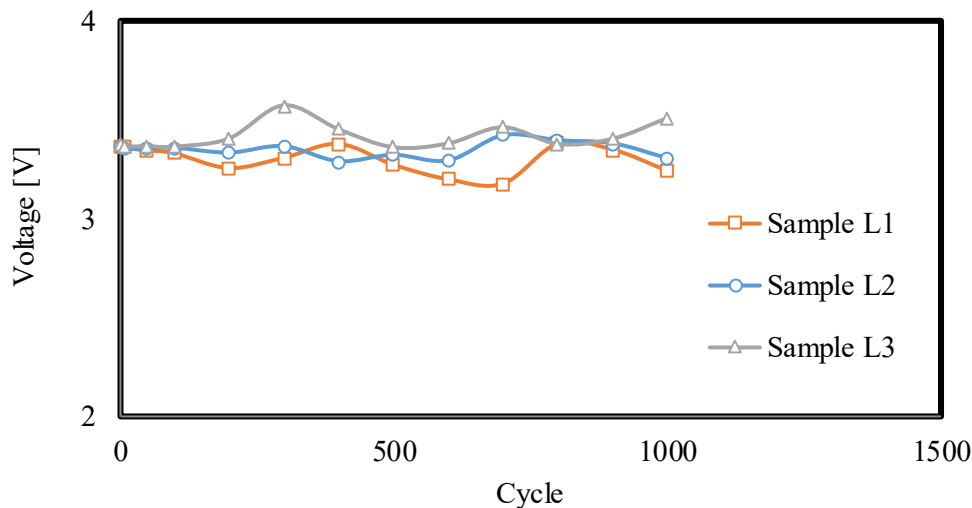


Figure 9. Battery voltage (End of mode cycle).

4 Discussion

4.1 AC impedance response in cycle durability test of Ni-MH^{[10], [11], [12], [13]}

Figure 10 shows the AC impedance measurement results for AB5 alloy-type Ni-MH experimental battery which is the most popular composite alloy structure of Ni-MH battery. Three sets of brand new batteries were used for cycle durability test. AC impedance measurement has been done first at the battery activation stage and then after reaching each checkpoint cycle: 100, 400, 700 and 1000. Ni-MH battery have 1900 mAh of rated capacity, is EVOLTA (model: HHR-3MWS), manufactured by Panasonic Co., Ltd. The experiment was carried out on brand-new batteries after activation by 10 charge-discharge cycles. The experimental test condition was the same of the Li-ion battery mentioned in section 2.6 (Experimental method). The rated capacity of the experimental Ni-MH battery (1900mAh) is different with the rated capacity of the experimental Li-ion battery (2150mAh). The experimental test was done that the charge-discharge cumulative capacity (Ampere-hour capacity) is not the same but the charge-discharge capacity rate (C rate) is the same in both experimental test.

Figure 10 shows that the AC impedance measurement results for AB5 alloy-type Ni-MH experimental battery was only increased electrolyte resistance (R_{sol}) over the course of durability test cycles. Figures 4-6 shows that the AC impedance measurement results for Li-ion experimental batteries were eventually increased electrolyte resistance (R_{sol}), charge transfer resistance (R_{ct}) and electric double layer capacitance (C_{dl}).

It is considered that additive material of electrode dissolves into electrolyte which is increased R_{sol} in Ni-MH battery. In Li-ion battery, it is considered that the SEI (solid electrolyte interface) is covered over electrode which is increased R_{ct} and C_{dl} . And, R_{sol} increases a little over the course of durability test cycles^{[14], [15]}.

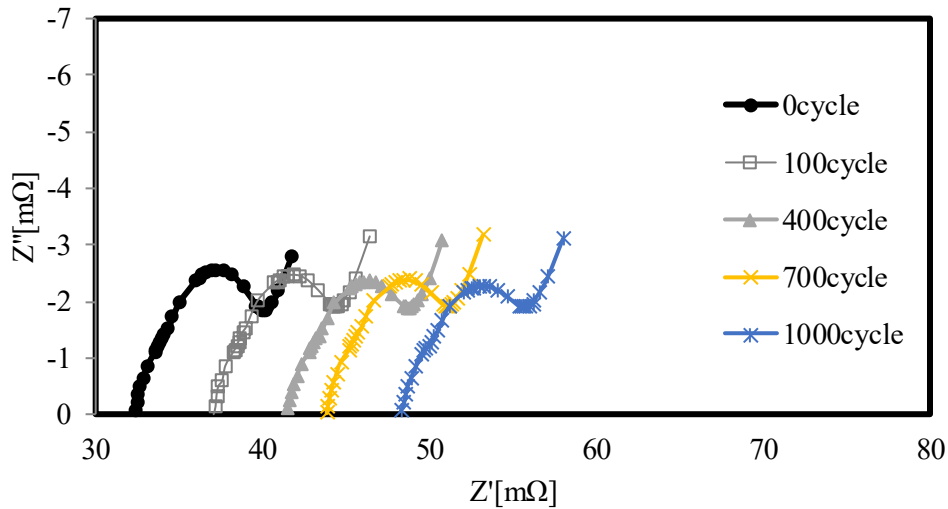


Figure 10. AC Impedance spectroscopy (Ni-MH).

5 Conclusion

In this study, Li-ion batteries were examined with durability cycle test and the following conclusions were made.

- (1) AC impedance response analysis, which method is available to verify Li-ion battery, applies to the battery deterioration condition in progress of cycle lifetime experiment.
- (2) High SOC range of 75/55%SOC is much affected deterioration than low SOC range of 33/13%SOC, which was 4.6 times (=5.1/1.1%) decreased from initial battery capacity in 1000 cycle.
- (3) AC impedance measurement results for AB5 alloy-type Ni-MH experimental battery was only increased electrolyte resistance (R_{sol}) over the course of durability test cycles. It is considered that additive material of electrode dissolves into electrolyte which is increased R_{sol} in Ni-MH battery.
- (4) AC impedance measurement results for Li-ion experimental batteries were eventually increased R_{sol} , charge transfer resistance (R_{ct}) and electric double layer capacitance (C_{dl}). In Li-ion battery, it is considered that the SEI (solid electrolyte interface) is covered over electrode which is increased R_{ct} and C_{dl} . And R_{sol} increases a little over the course of durability test cycles.

Acknowledgement

This study was partly sponsored by the Japan Society for Promotion of Science (JSPS) under the Grants-in-Aid for Scientific Research (No.16K06975 Battery stress control technology for electric prime movers).

References

- [1] Sakamoto, T., Matsuda, T., Minami, T., Evaluation of Hybrid Electric Vehicle Battery Life in North American Market, The 22nd International Battery, Hybrid and Fuel Cell Electric Vehicle Symposium & Exposition, <http://www.evs22.org/>, (2006)
- [2] Kameyama, H.; Study on Heat Generation Behavior at Small Lithium-ion Secondary Battery, JSME No.02-7 The 8th Symposium on Prime Mover and Energy Engineering, Tokyo, (2002), pp.387-392 (in Japanese)

- [3] Sakamoto, T.: Simulation of Battery SOC State of a Hybrid Electric Vehicle (Applying a Proposed Method of Road Inclination Convert to a Data Received by GPS), Transactions of the Japan Society of Mechanical Engineers, Series C, Vol.74, No.746, pp.2435-2442, (2008)
- [4] Mueller, J. M.; Characterization of Direct Methanol Fuel Cells by AC Impedance Response, Journal of Power Sources 75, (1998), pp.139-143
- [5] Itagaki, M.: Electrochemical Impedance Method, Maruzen, Tokyo, pp.61-62, (2011) (in Japanese)
- [6] Konomi, T.: Research on Diagnosis Technique on PEFC Running Condition, Transactions of the Japan Society of Mechanical Engineers, Series B, Vol.71, No.701, pp.245-250, (2005) (in Japanese)
- [7] Konomi, T.: Research on PEFC Overvoltage Analysis Method by Impedance Technique, Transactions of the Japan Society of Mechanical Engineers, Series B, Vol.72, No.723, pp.192-197, (2006) (in Japanese)
- [8] Tachibana, K.: Impedance Measurement Know-how and Data Analysis Method, Technical Information Association, Tokyo, pp.57-66, (2012) (in Japanese)
- [9] Sakamoto, T., Electric Load Analysis of a Hybrid Electric Vehicle (Commuting Monitor Beijing), Journal of Mechanical Systems for Transportation and Logistics, Vol.2, No.1 (2009), pp.66-77
- [10] Iwasaki, A., Todoroki, A., Shimamura, Y., Kobayashi, H.: Damage Identification by Discriminant Analysis Using Mahalanobis Distance (in Japanese), Transactions of the Japan Society of Mechanical Engineers, Series A, Vol.67, No.659, pp.1242-1247, (2001)
- [11] Nakatsugawa, M., Ohuchi, A.: A study on Determination of the Threshold in MTS Algorithm (in Japanese), Journal of Institute of Electronics Information and Communication Engineers, Vol.J84-A, No.4, p.520, (2001)
- [12] Takagi, Y., et al.: Evaluation for Life-expectancy Presumption Technique of Aged Switchboards Based on MTS Method (in Japanese), The transactions of the Institute of Electrical Engineers of Japan. D, A publication of Industry Applications Society, IEEJ transactions on industry applications, Vol.126, No.6, p.805, (2006)
- [13] Taguchi, G.: Mathematics for Quality Engineering, First version, pp.145-152, Japanese Standards Association, (1999)
- [14] Yoshida, H., Inamura, M., Inoue, T., et al., Verification of Life Estimation Model for Space Lithium-Ion Cells, Electrochemistry 78(5), pp.482-488, (2010)
- [15] Sakamoto, T., Japanese Unexamined Patent Application Publication No. JP-A-2015-94726, (2015)